Study of Muon Neutrino Oscillations Using MicroBooNE Data

Third Year Lab Report

Harry Tabb
Department of Physics and Astronomy, University of Manchester
(Experiment performed in collaboration with Maximilian Potts)
(Dated: April 27, 2023)

The aim of this experiment was to investigate neutrino oscillations using data from the MicroBooNE detector. The primary focus was to isolate muon neutrino signals from background events using selection cuts and machine learning techniques. By analysing energies of neutrino tracks, confidence regions were constructed for a two-flavour neutrino parameter space. These were propagated into a 3+1 model parameter space and were used to reject proposed parameters for a theoretical sterile neutrino by the LSND and MiniBooNE experiments.

1. INTRODUCTION

In this experiment, data from the MicroBooNE neutrino detector was used in conjunction with Monte Carlo generated data to investigate neutrino properties. The neutrino was first introduced by Pauli in 1930 to maintain conservation laws in beta decays [1]. David and Bahcall found that only one third of the predicted number of electron neutrinos produced by the sun were observed on earth [2]. This was known as the solar neutrino problem. In 1968 Pontecorvo theorised that neutrinos could oscillate between flavours which explained the measured deficit [3]. This was a shock to the field as this predicted that neutrinos have finite mass, contradicting the standard model. Since then, a plethora of experiments have been constructed to investigate neutrino oscillations such as the Super-Kamiokande (1996) and the Liquid Scintillation Neutrino Detector (LSND) (1993). However, the LSND experiment measured an excess of neutrino events at low energies. This is known as the Low Energy Excess (LEE). To account for this, a fourth neutrino flavour was theorised, once again going beyond the standard model. The study of neutrinos is fundamental to many areas of physics such as nuclear, particle and cosmology. Therefore, uncovering the theory behind neutrinos is imperative to understanding nature.

2. THEORY

In order to explain neutrino oscillations, neutrinos must have a finite mass as the theory requires the flavour eigenstates to be superpositions of mass eigenstates. The theory behind this is derived for the two flavour approximation and the 3+1 model in the next sections.

2.1. Two Flavour Approximation

In the two flavour approximation, the flavour states, $|\nu_\alpha\rangle$, are related to the mass states, $|\nu_i\rangle$, by

$$\begin{pmatrix} |\nu_e\rangle \\ |\nu_\mu\rangle \end{pmatrix} = \begin{pmatrix} \cos\theta & \sin\theta \\ -\sin\theta & \cos\theta \end{pmatrix} \begin{pmatrix} |\nu_1\rangle \\ |\nu_2\rangle \end{pmatrix} \tag{1}$$

where $\alpha = [e, \mu]$, $i = [1, 2]$ and θ is the mixing angle between the first and second flavour state. Therefore, the time propagation of a weak state can be represented by

$$|\nu_\alpha(t)\rangle = \exp\{iq_1 \cdot x\} \cos\theta \, |\nu_1\rangle + \exp\{iq_2 \cdot x\} \sin\theta \, |\nu_2\rangle \tag{2}$$

where q_i is the four momenta of the state i and x is the distance travelled. The probability that a neutrino of flavour α oscillates to a neutrino of flavour β after a time t is given by the inner product of the initial and final states

$$P(\nu_\alpha \to \nu_\beta) = |\langle \nu_\alpha(x,t) | \nu_\beta(0,0) \rangle|^2. \tag{3}$$

Therefore, by combining equations (2) and (3), this probability can be written in natural units as

$$P(\nu_\alpha \to \nu_\beta) = \sin^2 2\theta \sin^2 (1.27 \frac{\Delta m^2_{12} x}{E}) \tag{4}$$

where Δm^2_{12} is the difference between the squared masses of the mass states in eV, x is measured in km and E is the neutrino energy in GeV.

2.2. 3+1 Flavour Model

The 3+1 flavour model introduces a fourth sterile neutrino that doesn't interact via the weak force and has Δm^2_{14} of the order of 1eV. In this new model, the probability of oscillation is modified to

$$P(\nu_\alpha \to \nu_\beta) = 1 - 4(1 - |U_{\alpha 4}|^2)|U_{\beta 4}|^2 \sin^2 (1.27 \frac{\Delta m^2_{14} x}{E}) \tag{5}$$

and the relevant matrix elements for this experiment are given by

$$|U_{e4}|^2 = \sin^2 \theta_{14} \tag{6}$$

and

$$|U_{\mu 4}|^2 = \sin^2 \theta_{24} \cos^2 \theta_{14} \tag{7}$$

where θ_{ij} is the mixing angle between the states i and j [4]. By combining equations (5), (6) and (7) the following relation can be derived

$$\sin^2 2\theta_{\mu e} = \frac{\sin^2 2\theta_{14}}{1 + \sqrt{1 - \sin^2 2\theta_{14}}} [1 - \sqrt{1 - \sin^2 2\theta_{\mu\mu}}] \tag{8}$$

where $\theta_{\alpha\beta}$ represent mixing angles through the sterile neutrino and $\sin^2 2\theta_{14} = 0.24$ [5]. This equation is used to compare the 2 flavour approximation to the 3+1 model as θ_{12} is considered equal to $\theta_{\mu\mu}$.

3. EXPERIMENTAL APPROACH

The MicroBooNE experiment consists of a beam of muon neutrinos, created by colliding protons with a

beryllium target, incident on a liquid argon time projection chamber (LArTPC) [6]. Neutrinos cannot be detected directly as they do not interact with the electromagnetic force, therefore, neutrino interactions that emit charged particles are used to infer properties of the neutrino. For this experiment the ν_μ charged current interaction was of interest. The Feynman diagram for this is shown in Figure 1. Muon neutrinos interact with neutrons in the argon nuclei and produce muons and protons. These charged particles propagate through the liquid argon of the LArTPC and ionise argon atoms producing electrons and scintillation photons. These photons are used to trigger the detector to measure signal events. The electrons drift towards the detectors wire planes due to an applied electric field. This process is shown in Figure 2. The three wire planes allow for three dimensional reconstruction of particle tracks. From this the energy of the neutrino can be inferred.

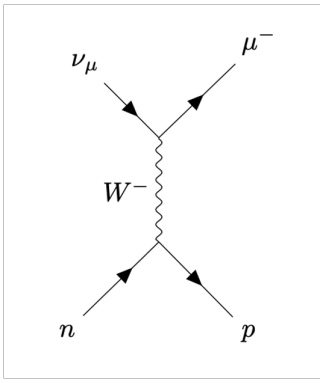

FIG. 1. A Feynman Diagram showing the signal event for this experiment. A muon neutrino interacting with a neutron with a W^- boson producing a muon and a proton.

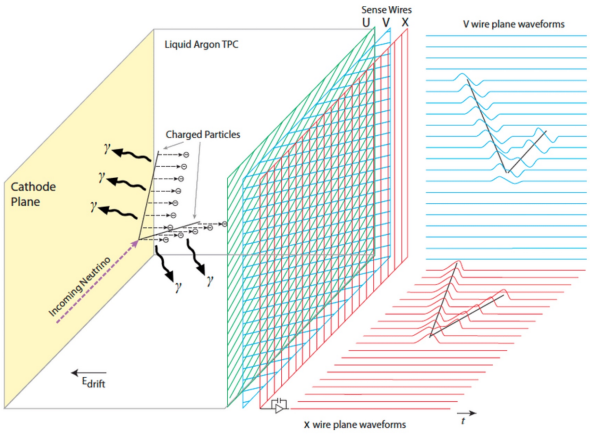

FIG. 2. A schematic diagram showing the interaction process along with the direction of the applied electric field and the three wire plane detectors [6].

A Monte Carlo simulation was used to simulate the signal and background events such as cosmic rays , ν_e charged current interactions and neutral current neutrino interactions. Distinct properties of the different events were used to make selection cuts to the data. For example, cosmic events tended to have a larger track length than the signal events. These cuts were then used to delete background events from the data set which improved the purity of the sample. The purer the data, the better it fits with the theoretical model. Random decision forests were used later in the experiment to improve the efficiency of the selection cuts (how much data is being removed). By increasing the size of the data set, it was less impacted by random fluctuations. A histogram of the energies of the events left in the data sets were then plotted against each other for analysis.

4. RESULTS

The original purity of the Monte Carlo data set was 72%. After the selection cuts were made, this increased to 90%, however, these cuts had an efficiency of 45% which meant over half of the data was being removed. The histogram of energies is shown in Figure 3. The simulation introduced a systematic error of 15% to the counts in the histogram. There was also a Poisson error on each bin in the histogram given by $\sqrt{N}$ where N is the counts in each bin. The simulation error was dominant for most of the bins due to a large number of counts, however; the Poisson error was relevant for the smaller bins. Machine learning was introduced to increase the efficiency of the cuts. The new efficiency was 68% whilst maintaining a purity of 90%. This meant that the counts in each bin of the histogram increased which made the Poisson error negligible for the whole experiment. A statistical test was also conducted on the histogram to find the largest amount of bins that could be used without over binning as this would introduce Poisson fluctuations. The largest amount of bins was desired as this would increase the number of degrees of freedom for the chi square analysis.

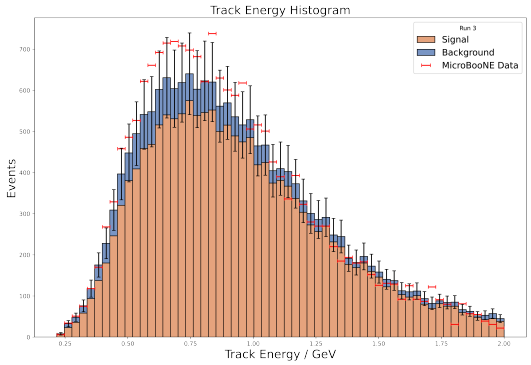

FIG. 3. A histogram of track energy for the Monte Carlo and the real MicroBooNE data. The Monte Carlo data is split into signal and background events.

It can be seen from Figure 3 that there is a discrepancy between the real data and the Monte Carlo simulation. This is because the simulation does not account for neutrino oscillations. Equation (4) for $\alpha = \mu$ and $\beta = e$ was applied to the Monte Carlo data for a range of $\sin^2\theta$ and m^2_{12} values and chi square test was conducted for each set of parameters. From this, a chi square contour plot was plotted for the range of parameter values as shown in Figure 4. Contours were drawn on the plot for chi square values corresponding to 90%, 95% and 99% confidence levels. The pa-

rameter space with a higher chi square value (right of the contour) could be rejected with the associated confidence. The experiment was not sensitive to the parameter space with lower chi square values (left of the contour). Therefore, these parameter values could not be rejected.

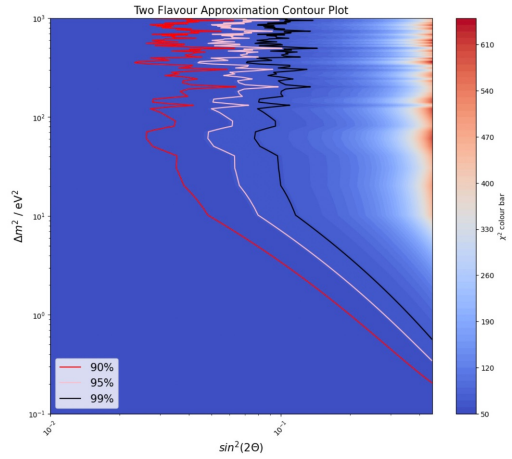

FIG. 4. A contour plot of chi square values for a range of $\sin^2 2\theta$ and Δm^2_{21} on a log scale. The plot contains three contour levels at the chi square values corresponding to 90% (red), 95% (pink) and 99% (black) confidence.

The $\sin^2(\theta)$ term in the two flavour approximation is approximated as $\sin^2(\theta_{\mu\mu})$ in the 3+1 model. Therefore, Equation (8) was used to propagate the chi square contour from the two flavour approximation into the 3+1 model. Using this new contour plot, the excluded regions were then compared to the sterile neutrino parameters proposed by LSND and MiniBooNE. This is shown in Figure 5. As the parameter space to the right of the contours can be rejected by this analysis, almost all proposed parameters were rejected at 90% confidence. However, only a small proportion were rejected at 99% confidence. To improve the sensitivity of this experiment more data is required. This could be achieved with a more sophisticated machine learning model to increase the efficiency of the selection cuts whilst maintaining a high efficiency. On top of this, more data could be acquired by increasing the amount of neutrino events measured. This could be achieved with a larger detector, replacing the liquid argon with a denser liquid or using a stronger neutrino beam. However, these were both beyond the limitations of the equipment. Collecting more data would increase both the efficiency and the purity of the data. Increasing the efficiency would decrease the random Poisson errors due. Increasing the purity would mean the data would align closer to the theoretical model as a higher proportion would be signal events. Despite not fully rejecting the 3+1 neutrino model, the parameter space was decreased substantially. Future neutrino detectors such as SBND and DUNE aim to implement these changes to further study the sterile neutrino.

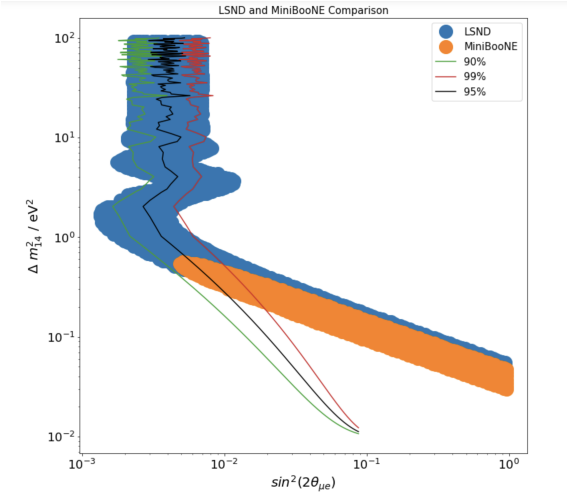

FIG. 5. A plot showing the sterile neutrino parameters proposed by the LSND and MiniBooNE experiments. Also on the plot are calculated chi square contours at 90% (green), 95% (black) and 99% (red) confidence.

5. CONCLUSION

In conclusion, almost all of the parameters for the sterile neutrino proposed by the LSND and MiniBooNE experiments were rejected at a 90% confidence level. As well as this, some parameters were also rejected at a 99% confidence level. This was achieved by using machine learning techniques to clean data from the MicroBooNE detector. Simulated Monte Carlo data was then fitted to the real data for a range of parameter values. Chi Square analysis was then used to reject parameter space. A larger parameter space could be rejected by increasing the size of the detector, using a stronger neutrino beam or implementing a more complex machine learning model. Future neutrino detectors such as DUNE aim to implement these improvements.

[1] T. Kajita, "Discovery of Neutrino Oscillations", *Reports on Progress in Physics*, **69**, page 1609, 2006
[2] J. Bahcall, R Davis, "Solar Neutrinos: A Scientific Puzzle", *Science*, **191**, pages 264-267, 1976
[3] B. Pontecorvo, "Neutrino Experiments and the Problem of Conservation of Leptonic Charge",*Sov. Phys. JETP*, **26**, pages 984-988, 1968
[4] M. Adams, et al, "Direct comparison of sterile neutrino constraints from cosmological data, ν_e disappearance data and $\nu_\mu \rightarrow \nu_e$ appearance data in a 3+1 model", *The European Physics Journal C*, **80**, page 2, 2020
[5] Mary Bisha, et al, "Search for a sterile neutrino in a 3+1 framework using the wire-cell inclusive charged-current ν_e selection from microboone" https://microboone.fnal.gov/ wp-content/uploads/MICROBOONE-NOTE-1116-PUB.pdf, 2022.
[6] R. Acciarri, et al, "Design and construction of the microboone detector" JINST, **12**, page 5, 2016.